Alginate oligosaccharides improve hepatic metabolic disturbance via regulating the gut microbiota

Yunchang Zhang [a,b], Xiong Deng [a], Tairan Liu [a], Baocheng Hu [a], Baoyi Yu [d], Linshu Jiang [a], Zhenlong Wu [b,c], Martine Schroyen [e], Ming Liu [a,e,*]

[a] College of Animal Science and Technology, Beijing University of Agriculture, Beijing, 102206, China
[b] State Key Laboratory of Animal Nutrition, Department of Animal Nutrition and Feed Science, China Agricultural University, Beijing, 100193, China
[c] Beijing Advanced Innovation Center for Food Nutrition and Human Health, China Agricultural University, Beijing, 100193, China
[d] College of Biological Sciences Engineering, Beijing University of Agriculture, Beijing, 102206, China
[e] Precision Livestock and Nutrition Unit, Gembloux Agro-Bio Tech, University of Liège, Gembloux, 5030, Belgium

ARTICLE INFO

ABSTRACT

Alginate oligosaccharides (AOS) derived from sodium alginate are novel prebiotics with multiple biological functions. Low birth weight (LBW) is a public health concern worldwide. However, the benefits of AOS in LBW mammals have not been determined. In this study, we found that AOS significantly improved the growth performance, colonic mucosal immunity, and jejunal nutrient digestion and transport of LBW piglets. Moreover, AOS alleviated liver injury by alleviating oxidative stress and pro-inflammatory responses, and improved hepatic lipid accumulation and insulin resistance by decreasing the levels of genes involved in lipid transport, *de novo* lipogenesis, and the insulin signaling. Integrated 16S rDNA, transcriptome, and metabolome analyses revealed that AOS alleviated the disruption of colonic mucosal immunity by increasing the abundance of *Lactobacillus* and short-chain fatty acids, and improved hepatic dysfunction via the tryptophan metabolites and aryl hydrocarbon receptor signaling. These findings revealed the effects and mechanisms of AOS in intestinal and hepatic dysfunction in LBW piglets, and broadened the potential application of AOS in improving postnatal maldevelopment in LBW infants.

1. Introduction

Intrauterine growth restriction (IUGR) is a prevalent public health concern worldwide with a 3–7% incidence in the total population and a high occurrence both in developing and developed countries (Romo, Carceller, & Tobajas, 2009). IUGR results from impaired growth and development of mammalian embryos or fetal organs during pregnancy, which ultimately leads to low birth weight (LBW) in infants and livestock, followed by delayed growth and permanent stunting during the postnatal lifetime (McMillen & Robinson, 2005; Wu, Bazer, Wallace, & Spencer, 2006). In addition, IUGR also results in high mortality and morbidity of neonates, making it an unneglected issue for human beings (Wu, et al., 2006). Among all mammals, neonatal piglets exhibit a natural prevalence of LBW and share similar growth and metabolic defects with LBW human neonates (Guilloteau, Zabielski, Hammon, & Metges,

2010; Roura et al., 2016), thus serving as an excellent model to investigate the underlying mechanism of IUGR occurrence both prenatally and postnatally, as well as for therapeutic options.

The intestines and liver are the main organs responsible for the digestion, absorption, and metabolism of dietary nutrients. Dietary nutrients must be hydrolyzed by digestive enzymes in the lumen of the small intestine before uptake and transport to the portal vein by corresponding transporters (Goodman, 2010). These nutrients, mainly carbohydrates and lipids, are then taken up by the liver for energy metabolism or synthesized as glycogen and triglycerides (Bechmann, et al., 2012; Jones, 2016; Postic, Dentin, & Girard, 2004). Accumulating evidence has shown that most of the LBW newborn mammals exhibited hepatic dysfunction, which is characterized by abnormal glucose and lipid metabolism, including insulin resistance and hepatic steatosis, sharing similar symptoms with clinical metabolic syndromes, such as type 2 diabetes, obesity, and other cardiovascular diseases (D. Chen

Abbreviations

ACC	acetyl-CoA carboxylase
ACSL1	adipose acyl-CoA synthetase 1
AGR2	anterior gradient 2
AhR	aryl hydrocarbon receptor
AKT2	AKT serine/threonine kinase 2
ALT	alanine transaminase
AMPK	AMP-activated protein kinase
AOS	alginate oligosaccharides
ASCT2	amino acid transporter 2
AST	aspartate transaminase
ATB$^{0,+}$	amino acid transporter B$^{0,+}$
CAT	catalase
CAV1	caveolin 1
CD36	cluster of differentiation 36
Chkα	choline kinase α
chREBP	carbohydrate response element binding protein
CPT1α	carnitine palmitoyltransferase 1α
DGAT2	diacylglycerol O-acyltransferase 2
EAAT3	excitatory amino acid transporter 3
ERN1	endoplasmic reticulum to nucleus signaling 1
FABPpm	plasma membrane fatty acid-binding protein
FASN	fatty acid synthase
FATP	fatty acid transport protein
FFA	free fatty acid
FOXO1	forkhead box O1
G6Pase	glucose-6-phosphatase
GLUT5	glucose transporter 5
GlyT1	glycine transporter 1
GPAT1	glycerol-3-phosphate acyltransferase 1
GPCPD1	glycerophosphocholine phosphodiesterase 1
GSK3	glycogen synthase kinase 3
GSTA4	glutathione s-transferase α 4
GYS2	glycogen synthase 2
HDL-C	high-density lipoprotein cholesterol
HK2	hexokinase 2
HO-1	heme oxygenase 1
IL-1β	interleukin 1β
INSR	insulin receptor
IUGR	intrauterine growth restriction
LBW	low birth weight
LDH	lactate dehydrogenase
LDL-C	low-density lipoprotein cholesterol
LXRα	liver X receptor alpha
MDA	malonaldehyde
Muc2	mucin 2
Myd88	myeloid differentiation factor 88
NBW	normal birth weight
NEFA	non-esterified fatty acid
Nrf2	nuclear factor erythroid 2-related factor 2
PCH	phosphoryl choline
PCK2	phosphoenolpyruvate carboxykinase 2
PFK1	phosphofructokinase 1
PYGL	glycogen phosphorylase L
PPAR	peroxisome proliferator activated receptor
rBAT	neutral and basic amino acid transport protein
SCFA	short-chain fatty acid
SGLT1	sodium/glucose cotransporter 1
SLC26A3	solute carrier family 26, member 3
SREBP1c	sterol regulatory element-binding protein 1c
TC	total cholesterol
TFF3	trefoil factor 3
TG	triglyceride
TLR	toll-like receptor
TNF-α	tumor necrosis factor α
T-SOD	total superoxide dismutase
y$^+$LAT2	y$^+$ ʟ-amino acid transporter 2

et al., 2022; Y. Liu, Azad, Kong, Zhu, & Yu, 2022; Mutamba, He, & Wang, 2022). In addition, the intestine is also the largest immune organ that protects against exogenous pathogens and antigens. Aberrant activation of intestinal mucosal immunity and chronic inflammation were also observed in LBW infants, which were represented by inductions of pro-inflammatory cytokines (Y. Li et al., 2018), loss of goblet cells (Huang, et al., 2020), impaired redox status (J. Chen et al., 2021), and decreased diversity of the microbial community (Zhang, et al., 2019), while restoring intestinal mucosal homeostasis guaranteed the "catch up" growth performance of LBW mammals (Cui, et al., 2022). Furthermore, lines of evidence revealed that the intestinal microbiota and relevant metabolites were significantly correlated with hepatic metabolic dysfunction failure (Hsu & Schnabl, 2023; Rao et al., 2021). In this scenario, postnatal nutritional strategies targeting the intestinal flora may serve as effective options for ameliorating hepatic metabolic dysfunction in LBW mammals.

Alginate oligosaccharides (AOS) are natural acidic polysaccharides derived from hydrolyzed alginate (Falkeborg, et al., 2014). Structurally, AOS consist of β-ᴅ-mannuronic acid (M) and α-ʟ-guluronic acid (G), which are linked by 1,4-glycosidic bonds in homogeneous or heterogeneous forms (Fischer & Wefers, 2019). Previous studies have reported AOS as a functional gelling, thickening or emulsifying agent in food industry (Gheorghita Puscaselu, Lobiuc, Dimian, & Covasa, 2020). However, AOS itself also show novel biological functions, including immunomodulatory, antioxidant, antiapoptotic, antimicrobial, antitumor, and antidiabetic effects (Houghton, et al., 2019; J. Liu et al., 2019). In particular, alginate is an indigestible polysaccharide and a source of dietary fiber (Brownlee, et al., 2005), which can function as a prebiotic by regulating the gut microbiota and producing short-chain fatty acids (SCFAs) (Yao, Kong, You, Zhong, & Hileuskaya, 2023). Lines of literature have also revealed the beneficial roles of AOS in the regulation of intestinal homeostasis, which was associated with inhibiting the release of pro-inflammatory cytokines, scavenging of reactive oxygen species (ROS), alleviating apoptosis of intestinal epithelial cells, decreasing the permeability of intestinal mucus, and restoring the microbial community (Jiang, et al., 2021; S. Lu et al., 2023; Mackie et al., 2016; Wan et al., 2018; Wan et al., 2021). However, whether AOS can alleviate intestinal dysfunction in LBW mammals still needs to be explored. In comparison with applications in intestines, only two studies have reported the functional roles of AOS in liver health (Y. Hao et al., 2023; S. Li, He, & Wang, 2019), and evidence regarding whether AOS can improve hepatic metabolic disturbance in LBW mammals is still lacking.

In the current study, we hypothesized that AOS could alleviate aberrant intestinal mucosal immunity and improve hepatic glucose and lipid metabolism by using the LBW piglet model. Moreover, in consideration of the health aspect of AOS as a dietary fiber, the beneficial effects in regulating hepatic metabolic disorders may be achieved by regulating the gut microbiota. The novel findings of our study may provide new insights into the biological functions of AOS in improving the growth restriction of LBW infants and convincing evidence for the underlying mechanisms involved, which may further broaden its applications as functional food supplement.

2. Materials and methods

2.1. Regents

Enzymatically degraded AOS was purchased from BZ Oligo Biotech Co., Ltd (purity >95%, Qingdao, China). The molecular weight (MW), M/G ratio, and degree of polymerization (DP) were 2.21 kDa, 1.6, and 2–5, respectively (Figs. S1A–C). Hematoxylin & eosin (H&E), Alcian blue (AB), and Alcian blue-periodic acid-Schiff (AB-PAS) staining kits were obtained from Solarbio Biotechnology Co. (Beijing, China). Assay kits for α amylase, sucrase, maltase, lipase, trypsin, alanine transaminase (ALT), aspartate transaminase (AST), lactate dehydrogenase (LDH), total superoxide dismutase (T-SOD), catalase (CAT), hydrogen peroxide (H_2O_2), and malonaldehyde (MDA), total cholesterol (TC), triglyceride (TG), non-esterified fatty acid (NEFA), high-density lipoprotein cholesterol (HDL-C), low-density lipoprotein cholesterol (LDL-C), glucose, and insulin were all purchased from Nanjing Jiancheng Bioengineering Institute (Nanjing, China). TRIzol and the FastQuant RT Kit (with gDNase) were products of TIANGEN Biotech (Beijing, China), and SYBR Premix Ex Taq II was purchased from Accurate Biotech (Hunan, China). The primers used were synthesized by Sangon Biotech Co. (Shanghai, China).

2.2. Experimental design

Piglets with a lower birth body weight by 10% were defined as LBW (Bauer, et al., 1998), which was used as a model of LBW infants, while piglets in each litter with heavier birth body weight than the average were identified as normal birth weight (NBW). All suckling piglets were weaned on day 21 and divided into four treatment groups, namely, NBW (NBW piglets fed a basal diet), NA (NBW piglets fed a basal diet containing 0.05% of AOS), LBW (LBW piglets fed a basal diet), and LA (LBW piglets fed a basal diet containing 0.05% of AOS). Each group consisted of 6 replicates with 6 piglets per replicate (n = 6). After supplementation with AOS for 28 continuous days, the piglets were euthanized for collection of blood, liver, jejunum, colon, and colon chyme samples. All experiments were approved by the Animal Care and Use Committee of Beijing University of Agricultural and conformed to the Guide for the Care and Use of Laboratory Animals (Approval number: BUA2023097).

2.3. Histological analysis

Colonic tissues fixed in 4% formaldehyde were dehydrated, embedded in paraffin, and sectioned. Sections were stained with H&E as instructed by the manufacturer and then visualized using a light microscope equipped with a computer-assisted morphometric system (Olympus AX80, Olympus Optical, Tokyo, Japan). Four sections were randomly examined, and representative images were taken.

2.4. Goblet cell counting

Colon sections were stained with AB or AB-PAS solution (blue) and nuclear fast red solution (red) according to the manufacturer's instructions (Solarbio, China). Sections from each piglet were visualized by a blinded observer and imaged using an Olympus AX80 microscope (Olympus Optical, Tokyo, Japan). The number of goblet cells was counted manually in 4 colonic crypts per section.

2.5. Biochemical index analysis

The serum levels of TC, TG, NEFA, HDL-C, LDL-C, glucose, insulin, H_2O_2, MDA, and activities of AST, ALT, LDH, T-SOD, and CAT were measured by the commercial kits according to the manufacturer's instructions. Homeostasis model assessment of insulin resistance (HOMA-IR) was calculated according to the formula, i.e., HOMA-IR = glucose level (mmol/L) × insulin level (mIU/L)/22.5 (Matthews, et al., 1985).

Liver homogenates were used for the detection of TC, TG, H_2O_2, and MDA levels, and T-SOD and CAT activities, while jejunum homogenates were used for the detection of α amylase, sucrase, maltase, and lipase activities. These results were normalized to the total protein concentrations in each sample. OD values were measured with a SpectraMax M3® spectrophotometer (Molecular Devices, Sunnyvale, CA).

2.6. Enzyme-linked immunosorbent assay (ELISA)

The concentrations of tumor necrosis factor α (TNF-α), interleukin 1β (IL-1β), IL-6, IL-17A, and IL-22 were measured by specific ELISA kits (Fankewei, Shanghai, China). The serum concentration was calculated according to the manufacturer's protocols, while the concentration in the colon was normalized to the total protein concentration.

2.7. Quantitative reverse transcription PCR (qRT-PCR)

Total RNA was extracted and reverse-transcribed into cDNA using TRIzol and FastQuant RT Kits (with gDNase) as instructed by the manufacturer (TIANGEN Biotech, Beijing, China). The RNA concentration and $OD_{260/280}$ value were measured using a Nanodrop P330 (Implen, Munich, Germany). The integrity of the total RNA was assessed by 1% agarose gel electrophoresis before qPCR experiments. qRT-PCR was performed using SYBR Premix Ex Taq II (Accurate, Hunan, China) and the LightCycler 96 System (Roche Diagnostics GmbH, Mannheim, Germany) according to the instructions of the manufacturers. GAPDH was used as an internal control. The $2^{-\Delta\Delta CT}$ method was used to determine the fold change in the mRNA level with the Microsoft Excel software. The primer sequences used were listed in Table S1.

2.8. 16S rDNA gene sequencing

Microbial genomic DNA was extracted from colonic chyme as instructed by the PowerSoil® DNA isolation kit (MoBio Laboratories, Carlsbad, CA, USA). DNA integrity was assessed by 1% agarose gel electrophoresis before amplification of the 16S rDNA V3–V4 gene region using the 338F and 806R primers. The PCR products were purified using the quick Gel Extraction Kit (Qiagen, Hilden, Germany) and were used for the construction of libraries with the Illumina TruSeq Nano DNA LT Library Prep kit. Paired-end sequencing was performed on a HiSeq2500 (Illumina, San Diego, USA). The raw data were screened, combined, and filtered into clean reads using QIIME (Version 1.9.1). The sequences with a similarity of 97% were grouped as operational taxonomic units (OTUs) and annotated using the SILVA 138 ribosomal RNA database.

The alpha diversity indices (Chao, Ace, Shannon, and Simpson) were calculated to reveal differences in the richness and diversity. Non-metric multidimensional scaling (NMDS) analysis based on the relative abundance of OTUs was performed to assess differences in the structure. Linear discriminant analysis (LDA) effect size (LEfSe) was used to examine the dominant taxa within each group. Student's t-test (P < 0.05) was used to identify the differential genera. The abovementioned analysis was performed on the online platform of Majorbio. Mantel's correlation was applied using the package "ggcor" in the R program. The relative abundances of candidate bacterial taxa (phyla and species) were analyzed using the provided sequence data to reveal changes in the bacterial community changes.

2.9. Hepatic transcriptome analysis

Total RNA was extracted from the liver tissues and quantified. The RNA-seq transcriptome library was prepared with an Illumina TruSeq™ RNA sample preparation kit (San Diego, CA), and sequenced with the a NovaSeq 6000 sequencer using a 2 × 150 bp paired-end configuration on an Illumina HiSeq X Ten platform. The trimmed and quality-controlled clean reads were separately aligned to the reference genome in orientation mode using HISAT2. The above procedures were

performed by Majorbio Biotechnology Co., Ltd. (Shanghai, China).

The expression level of each transcript was calculated following the transcripts per million reads (TPM) method to identify differential expression genes (DEGs). DEGs were then screened by DESeq2 with filter criteria of fold change (FC) ≥ 2 and q value < 0.05. Gene Ontology database (GO) and Kyoto Encyclopedia of Genes and Genomes (KEGG) database were used to identify which DEGs were significantly enriched at Benjamini-corrected p value < 0.05 by Goa tools and KOBAS 2.1.1 respectively. These analyses were performed on the Majorbio online platform.

2.10. Untargeted hepatic metabolome analysis

Hepatic metabolites were extracted with a 20% methanol solution containing internal standards. Each supernatant was transferred to an injection vial for liquid chromatography-mass spectrometry (LC-MS) analysis. Pooled quality control mixed with an equal volume of sample supernatant was also prepared. The samples were injected into a Thermo UHPLC-Q Exactive HF-X system equipped with an HSS T3 column (100 mm $\times$ 2.1 mm i.d., 1.8 μm; Waters, USA) at a flow rate and temperature of 0.4 mL/min and 40 °C respectively. The mobile phases consisted of 0.1% formic acid in water (mobile phase A) and 0.1% formic acid in acetonitrile: isopropanol (1:1, v/v) (mobile phase B). The mobile phase A changed as follows: 95-80-5-5-95-95% (0-3-9-13-13.1-16 min). The mobile phase B changed in response to A. The optimal conditions of MS equipped with electrospray ionization (ESI) were set as follows: source temperature at 425 °C, ion-spray voltage floating at -3500 V and 3500 V for negative and positive mode respectively, and normalized collision energy of 20–40-60 V. The detection was carried out over a mass range of 70–1050 m/z.

The acquired LC-MS data were processed and annotated with the HMDB, KEGG, and Metlin databases. KEGG enrichment analysis was carried out to investigate the metabolic enrichment and pathways, while KEGG topology analysis was performed to verify the most affected metabolic pathways. The relative abundances of candidate metabolites were analyzed using the provided sequence data. Differentially abundant metabolite screening was performed on the Majorbio Cloud platform.

2.11. Quantitative determination of short-chain fatty acids (SCFAs)

SCFA determination was performed as previously reported (Zhao, et al., 2022). Briefly, 0.5 g of colonic chyme was dissolved in 0.5 mL distilled water, and then mixed with 150 μL internal standard (4-methyl valeric acid, Sigma Aldrich, Saint Louis, MO, USA) and 0.1 mL of 25% phosphoric acid. The mixtures were then centrifuged and the supernatant was injected into a gas chromatograph (GC-7890B; Agilent Technologies, Wilmington, DE, USA) equipped with a flame ionization detector and a DB-FFAP capillary column (30 m $\times$ 0.25 mm $\times$ 0.25 μm; Agilent Technologies).

2.12. Statistical analysis

All the data were presented as the means $\pm$ SEMs and were analyzed with SAS software (SAS Institute Inc. Version 9.1) and Prism GraphPad (Version 9.0, GraphPad Software Inc., San Diego, CA, USA). Two-factor ANOVA or Student's *t*-test was used to analyze the data among the 4 treatment groups or 2 treatment groups. For two-factor ANOVA, the PROC general linear model was used for the interaction test, with body weight and AOS as the main factors. For data with unequal variance, the Mann-Whitney *U* test was used. *P < 0.05 and **P < 0.01 were considered statistically significant and statistically highly significant, respectively.

3. Results

3.1. AOS improved the health status and nutrients transport

The body weight of the LBW and LA groups were significantly lower than those of the NBW and NA groups ($P < 0.01$) (Fig. 1A) on day 24 and 37 after birth. The body weight of NA and LA groups were significantly greater than those of in the NBW and LBW groups on day 51 ($P < 0.05$) (Fig. 1A). AOS improved ADG in the NA and LA groups as compared with the NBW and LBW groups in the last 14 days and the whole 28 days ($P < 0.05$) (Fig. 1B). LBW piglets exhibited disruption of the jejunal mucosa in comparison with NBW piglets, which was improved by AOS, as demonstrated by the histological analysis (Fig. 1C). Compared with NBW piglets, the activities of α amylase, sucrase, maltase, and lipase were decreased in LBW piglets and were significantly reversed by AOS (Fig. 1D). In addition, AOS markedly upregulated the mRNA levels of *caveolin 1* (*CAV1*), *sodium/glucose cotransporter 1* (*SGLT1*), *SGLT3*, *glucose transporter 2* (*GLUT2*), *amino acid transporter 2* (*ASCT2*), and *y + L-amino acid transporter 2* (*y + LAT2*) in NBW piglets, and *CAV1*, *glycine transporter 1* (*GlyT1*), *neutral and basic amino acid transport protein* (*rBAT*), and *y + LAT2* in LBW piglets (Fig. 1E–G).

3.2. AOS improved the colonic mucosal immunity

No significant morphological changes in the distal colon were observed among the four treatment groups (Fig. 2A, upper panel). LBW piglets exhibited loss of goblet cells in comparison with NBW piglets, which was attenuated by AOS (Fig. 2A, middle and lower panel). In addition, statistical analysis also showed that AOS markedly increased goblet cell abundance in the colon of LBW piglets ($P < 0.01$) (Fig. 2B and C). Correspondingly, AOS largely increased the mRNA levels of genes encoding goblet cell-related cytokines, such as *mucin 2* (*Muc2*), *trefoil factor 3* (*TFF3*), *anterior gradient 2* (*AGR2*), *endoplasmic reticulum to nucleus signaling 1* (*ERN1*), *ERN2*, and *solute carrier family 26, member 3* (*SLC26A3*), but had no effect on *Muc4* expression ($P < 0.05$) (Fig. 2D). KEGG enrichment analysis of the colonic transcriptome revealed that the significant DEGs in response to AOS treatment were mainly involved in mucosal immunity, including infectious disease, signal transduction, immune system, and immune disease (Fig. 2E). Further analysis also revealed that AOS treatment led to marked reductions in pro-inflammatory cytokines, including TNF-α, IL-1β, IL-6, and IL-17A in both serum and the colon, and IL-22 in the colon (Fig. 2F and G).

3.3. AOS altered the colonic microbial community

No significant changes were observed in the alpha diversity of the colonic microbiota among the four treatment groups (Figs. S2A–D), while the PLS-DA results revealed marked separation in the colonic microbial structure (Fig. 3A). The relative abundances of Firmicutes, Bacteroidetes, and Actinobacteriota were not significantly different between NBW and LBW piglets (Fig. 3B, Figs. S2E). AOS treatment increased Firmicutes while markedly reduced Bacteroidetes abundance (Fig. 3C and D), resulting in significant increase in the ratio of Firmicutes to Bacteroidetes (Fig. 3E). The LEfSe analysis revealed that *Clostridium_sensu_stricto_1*, *Prevotellaceae_UCG-001*, *Actinomyces*, *Intestinibacter*, *Amnipila*, *Frisingicoccus*, and *Corynebacterium* were enriched in LBW piglets, whereas *Lactobacillus*, *NK3A214_group*, *Eubacterium*, *Anaerofustis*, *Butyrivibrio*, *Acidaminococcus*, *Enterorhabdus*, *Libanicoccus*, and *Peptococcus* were enriched in AOS-treated LBW piglets (Fig. 3F). At the genus level, AOS treatment significantly increased the relative abundances of *Lactobacillus*, *NK3A214_group*, *Anaerofustis*, *Enterorhabdus*, and *Peptococcus* in the colon of LBW piglets (Fig. 3G). Among all the *Lactobacillus* species detected, *Lactobacillus amylovorus* (*L. amylovorus*) was markedly promoted, while *L. reuteri*, *L. mucosae*, and *L. salivarius* only displayed increasing trends (Fig. 3H–K). Furthermore, Mantel's correlation analysis showed that bacteria enriched in piglets in
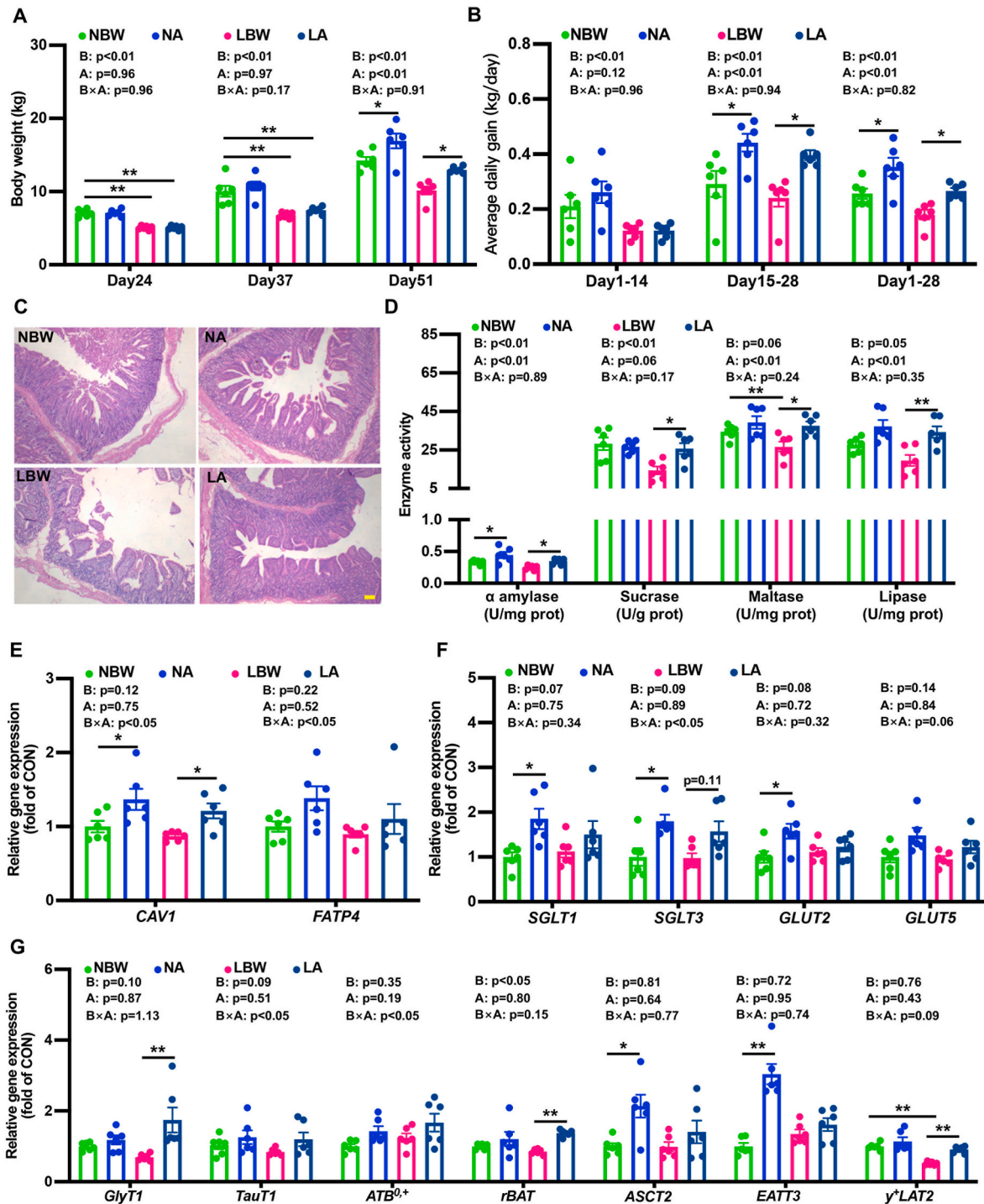
Fig. 1. AOS improved the health status and jejunal digestion and absorption of dietary nutrients. (A) Body weight on day 24, 37, and 52 after birth. (B) ADG from day 24–37, 38–51, and 27–51. (C) Representative H&E staining images of jejunum tissues. The scale bar represents 100 μm. (D) Activities of jejunal digestive enzymes. (E–G) Relative gene expression of lipid, glucose, and amino acid transporters. GAPDH was used as a reference gene. Statistical significance was determined by 2-factor ANOVA, B = body weight, A = AOS, *P < 0.05, **P < 0.01.

the LBW and LA groups had negative and positive relationships with final body weight and ADG from days 38–51 and 24–51, respectively (Fig. 3L).

3.4. AOS enhanced SCFAs and SCFA-producing bacteria

AOS treatment dramatically increased the abundances of acetate, propionate, butyrate, valerate, isobutyrate, isovalerate, and total SCFAs

(Fig. 4A–E, Figs. S3A and B), as well as SCFA-producing bacteria, including *Lactobacillus* and *Eubacterium* (Fig. 4F). AOS also promoted the relative abundances of *Prevotella*, *Ruminococcus*, *Lachnospiraceae_NK4A136_group*, *Coprococcus*, *Butyrivibrio*, *Faecalibacterium prausnitzii* (*F. prausnitzii*), *Eubacterium rectale* (*E. rectale*), and *E. hallii*, which can also produce SCFAs (Fig. 4F). Regression analysis revealed significant linear relationships between SCFA concentration and the relative abundance of *Lactobacillus* and L. *amylovorus* (Fig. 4G, H, Figs. S3C and
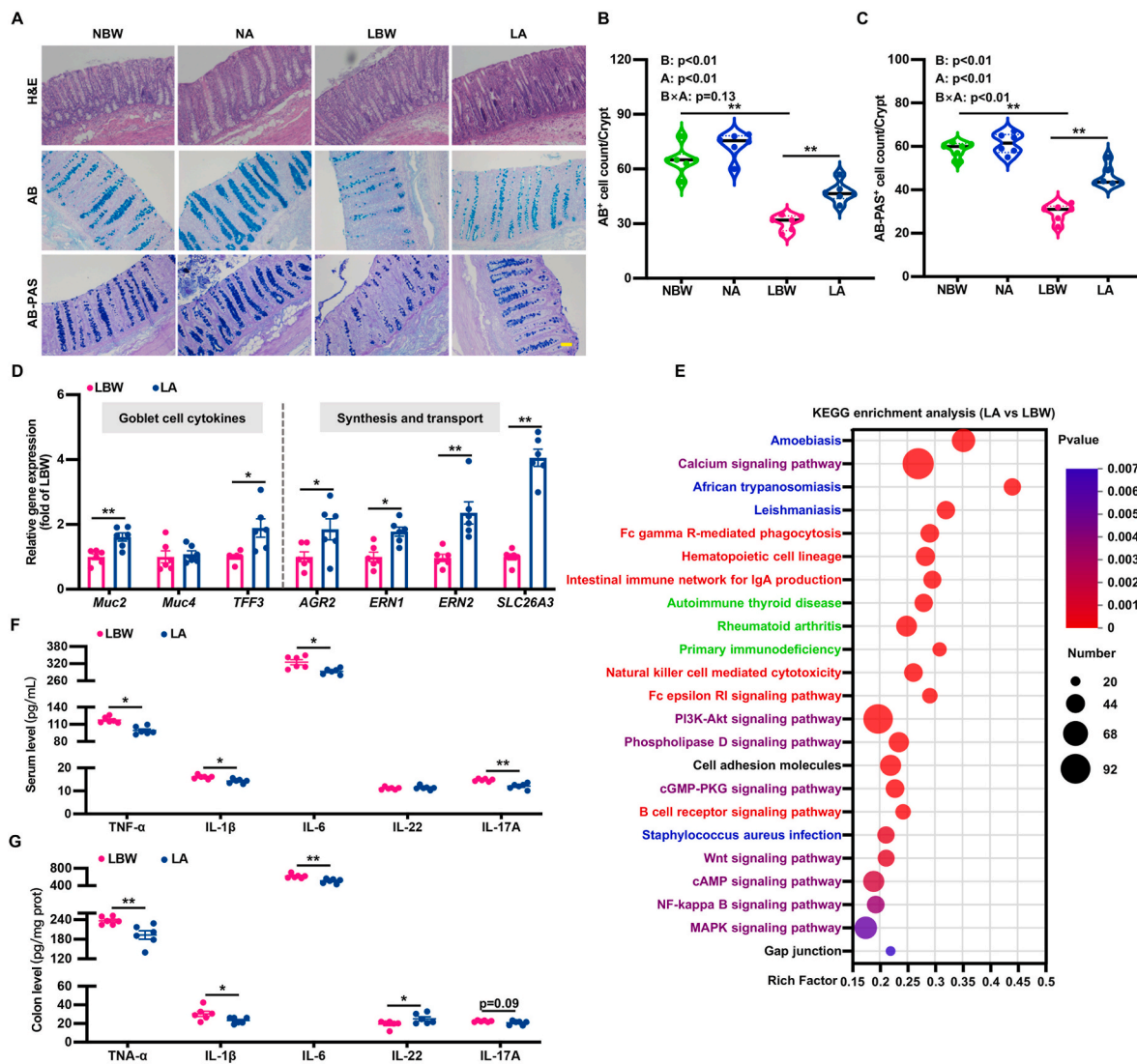
Fig. 2. Attenuation of colonic mucosal immunity by AOS. (A) Representative H&E (upper panel), AB (middle panel), and AB-PAS (lower panel) staining images of colon tissues. The scale bar represents 100 μm. (B, C) Statistical analysis of AB⁺ and AB-PAS⁺ cells. (D) Relative gene expression of cytokines secreted by goblet cells. (E) Bubble diagram of enriched KEGG pathways. The size of the dots represents the number of genes in each KEGG pathway. Blue, purple, red, and green represent infectious disease, signal transduction, immune system, and immune disease respectively. (F–G) Serum and colon levels of TNF-α, IL-1β, IL-6, IL-22, and IL-17A. Statistical significance was determined by 2-factor ANOVA and Student's *t*-test, B = body weight, A = AOS, *P < 0.05, **P < 0.01.

D). In addition, bacteria enriched in LBW piglets treated with or without AOS showed a positive or negative relationship with SCFA concentration, which further showed a negative or positive relationship with TNF-α, IL-1β, IL-6, and IL-17A in the serum and colon (Fig. 4I).

3.5. AOS altered hepatic glucose and lipid metabolism

LBW piglets exhibited increased serum ALT, AST, and LDH activities when compared with NBW piglets, which were significantly attenuated by AOS (Fig. 5A–C). GO functional enrichment analysis of the hepatic transcriptome between the LBW and LA treatment groups revealed that the TOP50 enrichment items were biological processes (Figs. S4A), most of which involved lipid, carbohydrate, and amino acid metabolism, with lipid metabolism being the most enriched (Fig. 5D and E). Further exploration found that TG and TC in the serum and liver, and NEFA, glucose, insulin, and HOMA-IR were increased in LBW piglets, all of which were alleviated by AOS (Fig. 5F-M). The serum levels of LDL-C and HDL-C were increased and decreased in LBW piglets respectively, and these changes were reversed by AOS (Figs. S4B and C).

The hepatic transport and metabolism of glucose and lipids were

presented in Fig. 6A. Most of the genes downregulated by AOS were enriched in glucose and lipid metabolism, including steroid hormone biosynthesis, glycerolipid metabolism, fatty acid degradation, regulation of lipolysis in adipocytes, and glycolysis or gluconeogenesis (Fig. 6B). Further analysis revealed that piglets treated with AOS showed significantly reduced mRNA levels of *CAV1, cluster of differentiation 36* (*CD36*), *FATP5* (free fatty acid (FFA) transporter), *adipose acyl-CoA synthetase 5* (*ACSL5*), *fatty acid synthase* (*FASN*), carbohydrate response element binding protein (*chREBP*), *sterol regulatory element-binding protein 1c* (*SREBP1c*) (fatty acyl-CoA synthesis), *glycerol-3-phosphate acyltransferase 1* (*GPAT1*), *GPAT4*, *diacylglycerol O-acyltransferase 2* (*DGAT2*) (TG synthesis), and *choline kinase α* (*Chkα*) (phosphoryl choline (PCH) synthesis), decreased trends in *plasma membrane fatty acid-binding protein* (*FABPpm*), *FATP2, ACSL1, acetyl-CoA carboxylase* (*ACC*), and *glycerophosphocholine phosphodiesterase 1* (*GPCPD1*), and increased trends in *carnitine palmitoyltransferase 1α* (*CPT1α*) and *CPT2* (Fig. 6C). AOS treatment also decreased the mRNA levels of *SLC2A2, SLC2A4,* and *SLC5A10* (glucose transporter), *glycogen synthase kinase 3α* (*GSK3α*), *GSK3β*, and *glycogen synthase 2* (*GYS2*) (glycogen synthesis), *hexokinase 2* (*HK2*) and *phosphofructokinase 1* (*PFK1*) (glycolysis), and
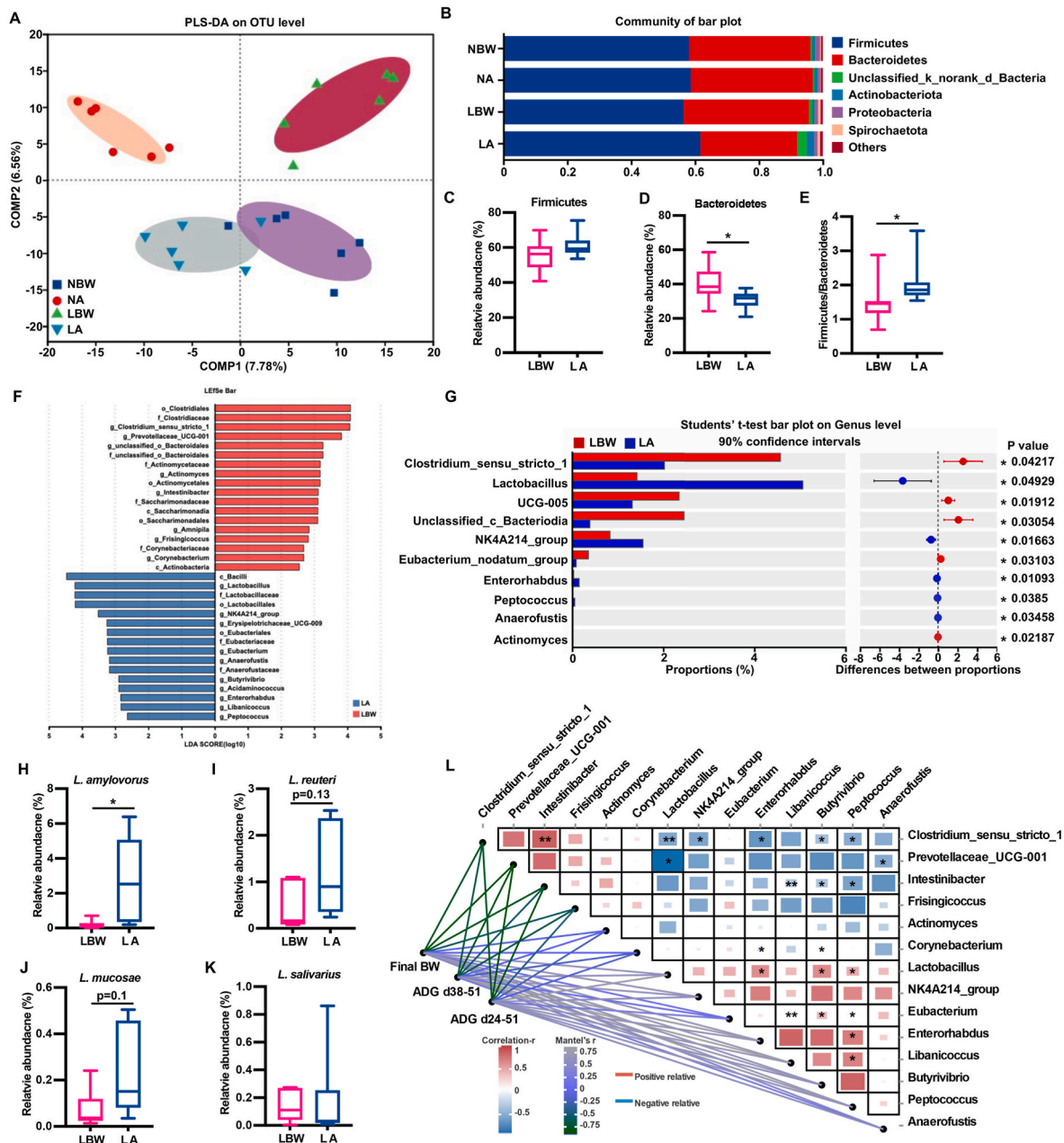
Fig. 3. Regulatory roles of AOS in the colonic microbial community. (A) PLS-DA diagram of the microbial structure. (B) Community of the bar plot at the phylum level. (C, D) Relative abundance of Firmicutes and Bacteroidetes. (E) The ratio of Firmicutes to Bacteroidetes. (F) LEfSe analysis of enriched taxa between the LBW and LA treatment groups. (G) The TOP10 significantly differentially abundant bacteria at the genus level. (H–K) Relative abundances of *L. amylovorus*, *L. reuteri*, *L. mucosae*, and *L. salivarius*. (L) Pairwise comparisons of differentially abundant taxa. The color gradient denotes Spearman's correlation coefficients. Bodyweight and ADG were related to taxa by the partial Mantel test. The edge color denotes the statistical correlation. The relative abundances of Bacteroidetes and *L. amylovorus*, and ratio of Firmicutes/Bacteroidetes were determined by Mann-Whitney U test while the others were determined by Student's *t*-test, *$P < 0.05$, **$P < 0.01$.

upregulated the mRNA levels of *glycogen phosphorylase L* (*PYGL*) (glycogenolysis), *glucose-6-phosphatase* (*G6Pase*), and *phosphoenolpyruvate carboxykinase 2* (*PCK2*) (gluconeogenesis) (Fig. 6D). AOS also decreased the expression of genes involved in pyruvate metabolism, the citrate cycle, the peroxisome proliferator activated receptor (PPAR) signaling pathway, and the insulin signaling pathway as shown by KEGG enrichment analysis (Fig. 6E), which were further identified by reductions in mRNA levels of lipid and glucose regulatory elements, including *PPARα*, *PPARγ*, *liver X receptor α* (*LXRα*), *insulin receptor* (*INSR*), *AKT serine/threonine kinase 2* (*AKT2*), and *forkhead box O1* (*FOXO1*) (Fig. 6F and G).

3.6. AOS improved hepatic tryptophan metabolites

The KEGG enrichment and KEGG topology analyses of hepatic metabolic profiles showed that tryptophan metabolism signaling was significantly affected by AOS (Fig. 7A and B). In addition, KEGG enrichment analysis of hepatic transcriptional revealed that most of the genes involved in tryptophan metabolism were downregulated (Figs. S4D). Furthermore, 8 kinds of tryptophan metabolites, including 5-hydroxy-tryptophan, quinoline-4,8-diol, xanthurenic acid, 3-indole-acetic acid, 3-methylindole, (E)-indol-3-ylacetaldoxime, indole-3-acetamide, and N′-formylkynurenine, were strongly upregulated in the liver by AOS (Fig. 7C). Hepatic tryptophan metabolites exhibited a negative correlation with hepatic TC and a significant negative
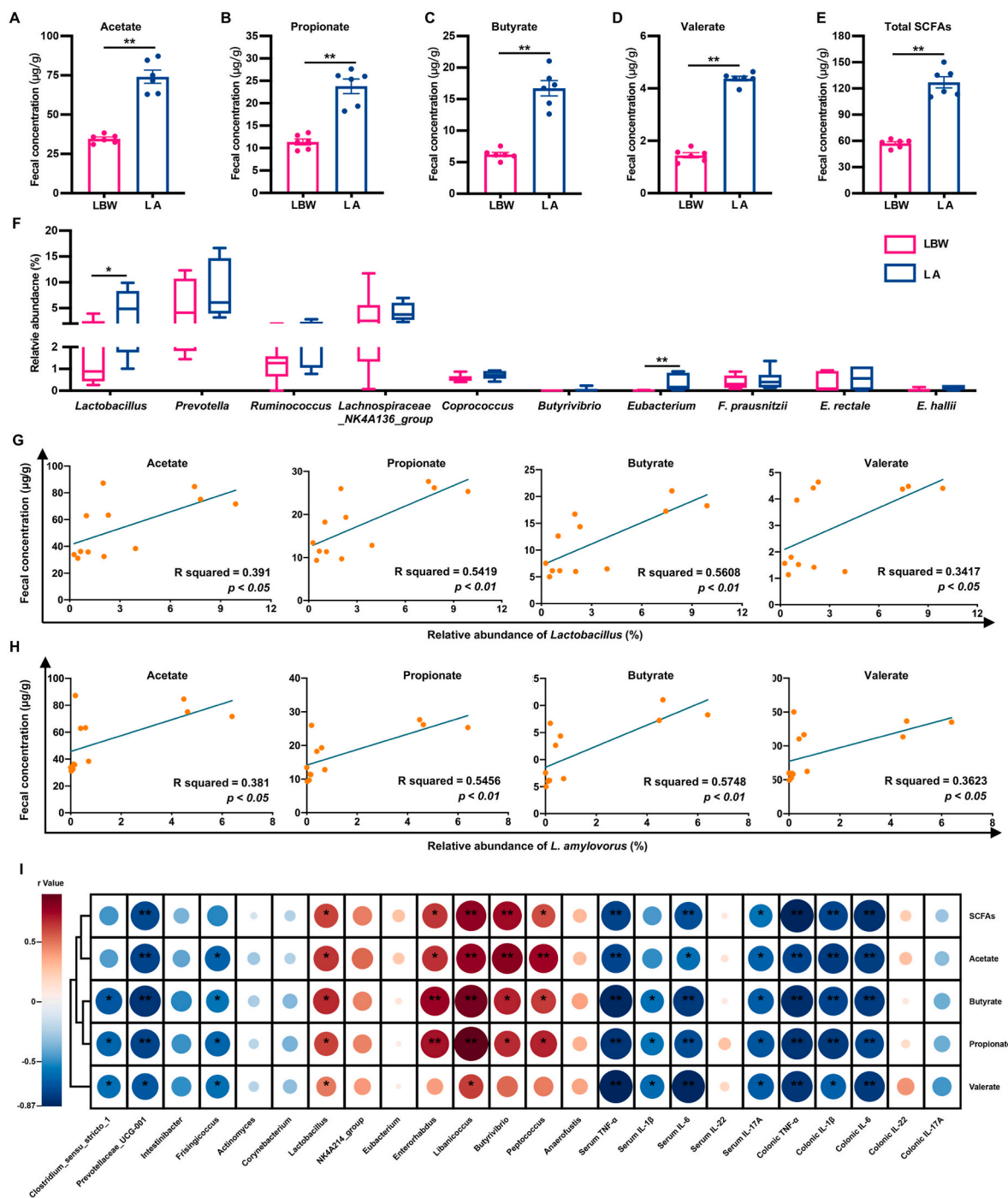
Fig. 4. Enhanced effects of AOS in SCFAs and SCFA-producing bacteria. (A–E) Concentrations of acetate, propionate, butyrate, valerate, and total SCFAs in the colonic chyme. (F) Relative abundance of SCFA-producing bacteria. (G, H) Association of SCFA concentration with the relative abundance of *Lactobacillus* and L. *amylovorus*. (I) Spearman correlation between the concentration of SCFAs and bacterial taxa enriched in LBW piglets treated with or without AOS, and serum and colon levels of pro-inflammatory cytokines. Statistical significance was determined by Student's *t*-test, *P < 0.05, **P < 0.01.

correlation with hepatic TG and serum TC, TG, NEFA, glucose, insulin, and HOMA-IR (Fig. 7D).

3.7. AOS alleviated hepatic dysfunction via aryl hydrocarbon receptor (AhR) signaling

According to the results of hepatic transcriptional KEGG analysis, genes downregulated by AOS were enriched in ROS related carcinogenesis, inflammatory mediator regulation of tryptophan channels, ferroptosis, Toll-like receptor (TLR), and the IL-17A signaling pathways

(Fig. 8A). AOS treatment increased the mRNA levels of *AhR, cytochrome P450 family 1 subfamily A member 1* (*Cyp1α1*), and *Cyp1α2* (AhR signaling), *nuclear factor erythroid 2-related factor 2* (*Nrf2*), *heme oxygenase 1* (*HO-1*), and *glutathione s-transferase alpha 4* (*GSTA4*) (Nrf2 signaling), and decreased the mRNA levels of *TLR4* and *myeloid differentiation factor 88* (*Myd88*) (TLR signaling) (Fig. 8B). Additionally, AOS decreased the hepatic and serum levels of MDA and H_2O_2, and the mRNA levels of *TNF-α, IL-1β, IL-17A, IL-6*, and *IL-22*, while increased the levels of CAT and T-SOD (Fig. 8C–K). Spearman correlation analysis revealed that hepatic tryptophan metabolites exhibited a positive
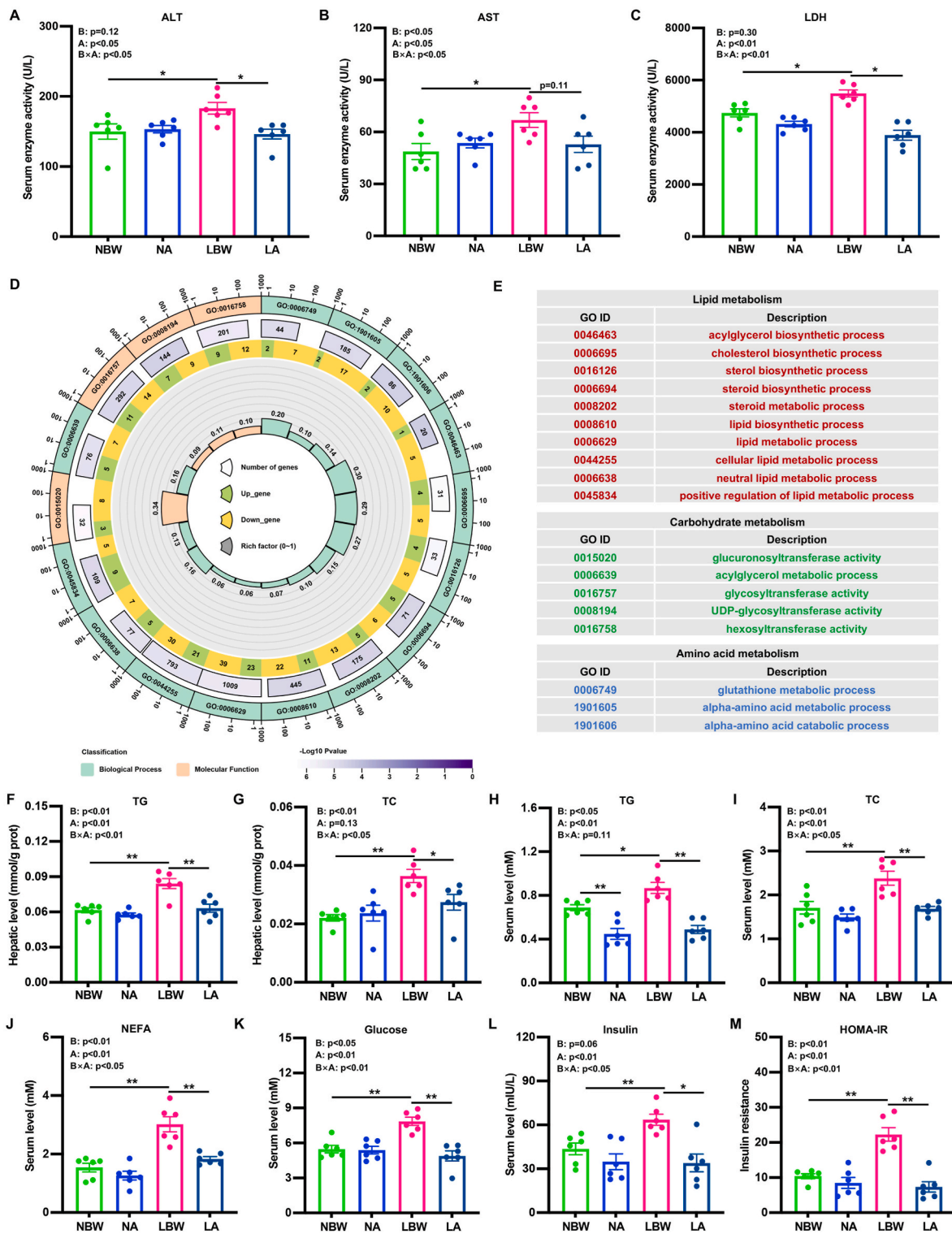
Fig. 5. The altered hepatic metabolic profiles by AOS. (A–C) Activities of serum ALT, AST, and LDH. (D–E) Circle plot of GO enrichment based on the hepatic transcriptome. The TOP50 GO items related to lipids, carbohydrates, and amino acids were listed. (F, G) Hepatic levels of TG and TC. (H–L) Serum levels of TG, TG, NEFA, glucose, and insulin. (M) HOMA-IR index calculated by the formula: HOMA-IR = glucose level (mmol/L) × insulin level (mIU/L)/22.5. Statistical significance was determined by 2-factor ANOVA and Student's t-test, B = body weight, A = AOS, *P < 0.05, **P < 0.01.

relationship with the antioxidative system including CAT, T-SOD, and Nrf2 signaling, and a negative relationship with LDH, MDA, H_2O_2, and mRNA levels of pro-inflammatory cytokines (Fig. 8L).

4. Discussion

AOS has demonstrated various biological properties and thus has been used in various diseases. Particularly, as a novel kind of prebiotic, AOS has been applied in treating inflammatory intestinal dysfunction. However, evidence regarding the regulatory role of AOS in intestinal
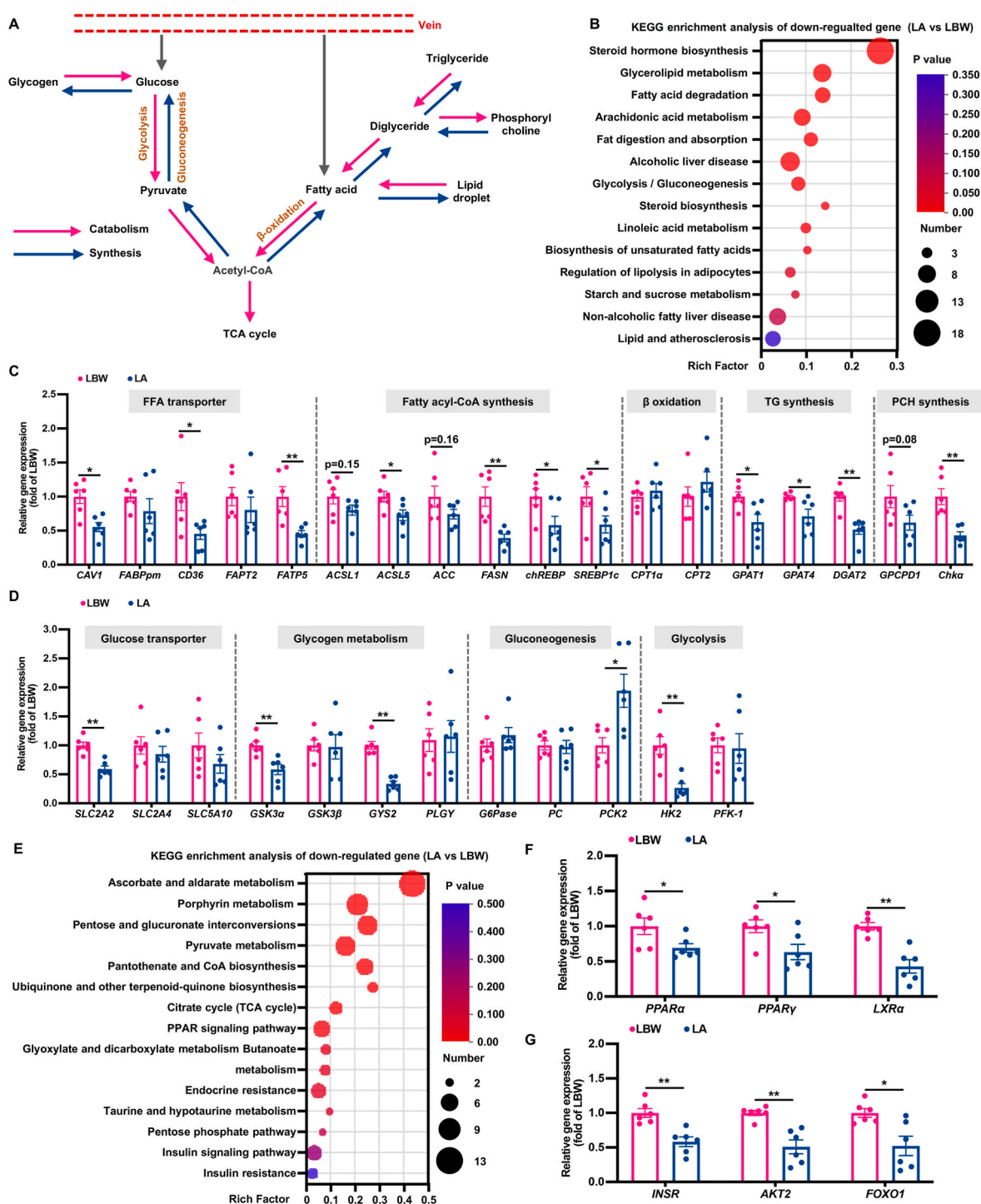
Fig. 6. Altered hepatic glucose and lipid metabolism by AOS. (A) Conclusive map of hepatic uptake and metabolism of glucose and lipids. (B) Bubble diagram of enriched KEGG pathways. The size of the dots represents the number of downregulated genes involved in hepatic glucose and lipid metabolic pathways. (C) The relative expression of genes involved in FFA transport, fatty acyl-CoA synthesis, β oxidation, and *de novo* synthesis of TG and TC. (D) The relative expression of genes involved in glucose transport, glycogenesis, glycogenolysis, gluconeogenesis, and glycolysis. (D) Bubble diagram of enriched KEGG pathways. The size of the dots represents the number of downregulated genes involved in energy metabolism. (F, G) Relative expression of genes encoding *de novo* lipogenesis and insulin resistance. GAPDH was used as a reference gene. *GPAT4* expression was determined by Mann-Whitney *U* test while the others were determined by Student's *t*-test, *P < 0.05, **P < 0.01.

and hepatic dysfunction in LBW infants has yet to be determined. In the current study, we found that AOS improved intestinal and hepatic dysfunctions by using a LBW piglet model. The mechanisms responsible for these positive outcomes were related to the regulation of the gut microbiota and microbial metabolites, especially the genera of *Lactobacillus*, SCFAs and tryptophan metabolites. Our study has revealed the functional properties of AOS in improving growth performance, elucidated the mechanisms of AOS in LBW-associated intestinal and hepatic dysfunction, and broadened the potential application of AOS in improving postnatal maldevelopment of LBW infants for the first time.

The dosage of AOS in the present study was based on our pilot study, which showed that 0.05% of AOS could significantly increase body
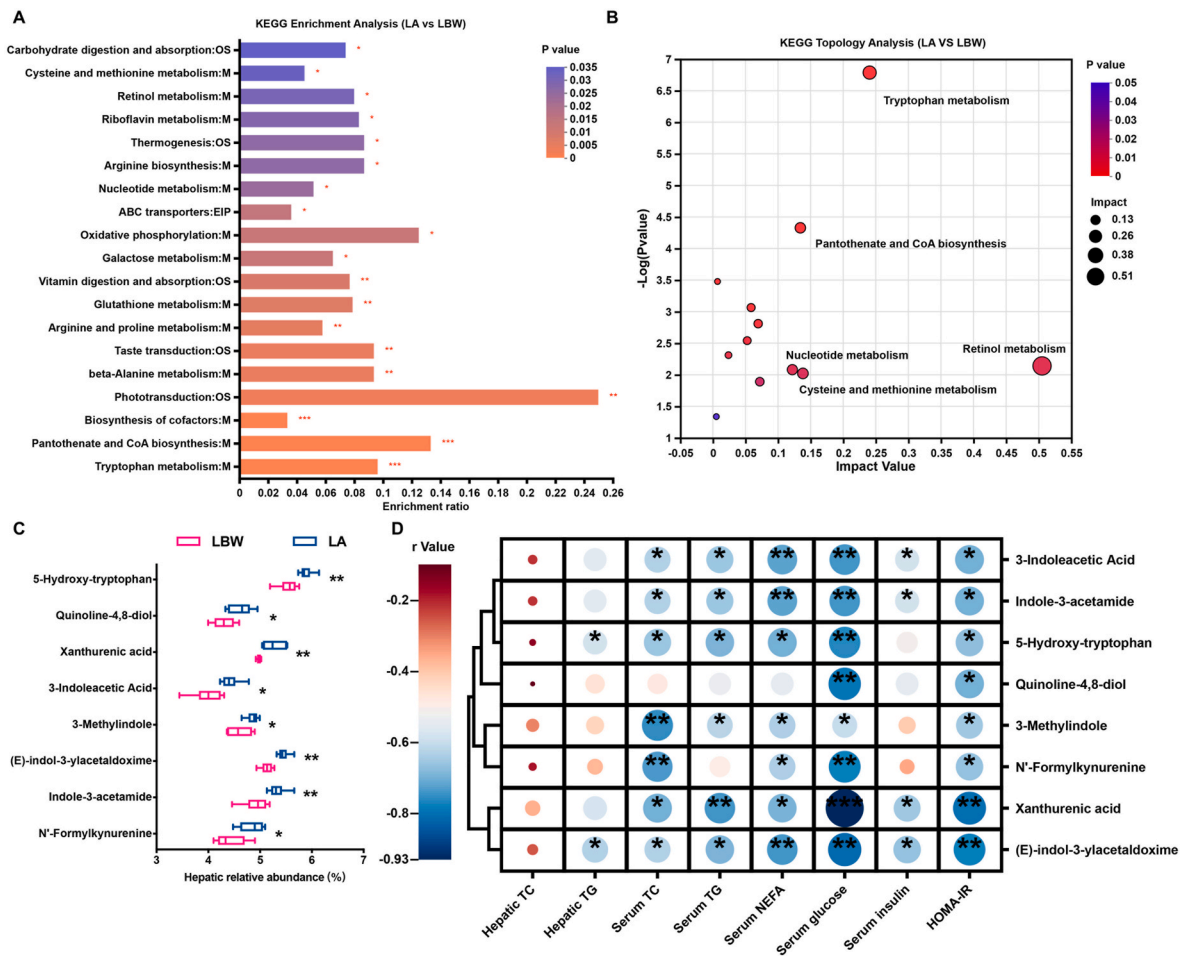
Fig. 7. Altered hepatic tryptophan metabolism by AOS. (A, B) KEGG enrichment and topology analysis based on the hepatic metabolome. (C) The relative abundance of candidate tryptophan metabolites. (D) Spearman correlation between the relative abundance of tryptophan metabolites and indices for hepatic glucose and lipid metabolism. Statistical significance was determined by Student's *t*-test, *P < 0.05, **P < 0.01.

weight and alleviate intestinal oxidative stress in weaning piglets. Feeding intolerance is commonly observed in LBW infants (Bozzetti, Tagliabue, Visser, van Bel, & Gazzolo, 2013; Neu & Zhang, 2005), and may directly lead to a reduction in growth performance. Our results showed that AOS greatly increased the experimental body weight and ADG of piglets, showing benefits in growth performance in LBW piglets. The small intestines, especially the jejunum, are the main sites for digestion and absorption of dietary nutrients. The absorption of nutrients depends on corresponding transporters on the membrane of intestinal epithelial cells located in the villus (Sundaram & Borthakur, 2021). However, most of the LBW infants suffer from impaired or delayed development of the small intestine, and decreased nutrient utilization efficiency (Ayuso, Irwin, Walsh, Van Cruchten, & Van Ginneken, 2021; Wang et al., 2014; Wellington et al., 2021). In the current study, LBW piglets exhibited disrupted jejunal morphology and lower activities of α amylase, sucrase, maltase, lipase, and trypsin. AOS increased the activities of these enzymes and transcriptional levels of dietary glucose, lipids, and amino acids, and protected the integrity of the jejunal morphology of LBW piglets, which may be responsible for the induction of growth performance.

The intestines are also the largest immune organ, whose homeostasis is quite crucial for maintenance of the health of the host. Goblet cells residing throughout the intestines are responsible for synthesizing biological macromolecules, including mucins and TFF3, to support the intestinal chemical barrier functions (Gustafsson & Johansson, 2022). Loss of goblet cells and reductions in mucins were reported in LBW piglets (Huang, et al., 2020). In the current study, AOS increased goblet cells in

LBW piglets but not in NBW piglets. Furthermore, AOS prevented the loss of goblet cells and improved the secretion of biological macromolecules in goblet cells. Additionally, lines of literature reported the aberrant activation of colonic inflammatory responses characterized by increased levels of pro-inflammatory cytokines in LBW piglets, while the "catch-up" performance was associated with the inactivation of inflammatory responses (Cui, et al., 2022). The results of colonic RNA-sequencing showed that most of the genes downregulated by AOS were enriched in mucosal immunity, which was further evidenced by decreased TNF-α, IL-1β, IL-6, and IL-17A both in the serum and the colon. AOS has been shown to relieve intestinal inflammation in piglets and mice (S. Lu et al., 2023; Wan et al., 2021). Our study shares similarities with these reports.

The previous study reported no significant differences in the microbial diversity between NBW and LBW piglets at any stage (N. Li, Huang, et al., 2018). In agreement with the findings of this study, the alpha diversity did not differ between NBW and LBW piglets regardless of treatment with or without AOS. A significant separation was observed among the four treatment groups in the current study, indicating that AOS altered the microbial structure of LBW piglets. Further analysis revealed that AOS markedly increased the Firmicutes/Bacteroides ratio, the decrease in which was reported as a relevant marker of gut dysbiosis in inflammatory bowel disease (Stojanov, Berlec, & Štrukelj, 2020). The alleviation of colitis by prebiotics is closely related to modification of the gut microbiota and microbial metabolites (Roy & Dhaneshwar, 2023). LEfSe analysis revealed that the genera of *Lactobacillus* and *Eubacterium*, both of which can produce SCFAs in the colon (Markowiak-Kopeć &
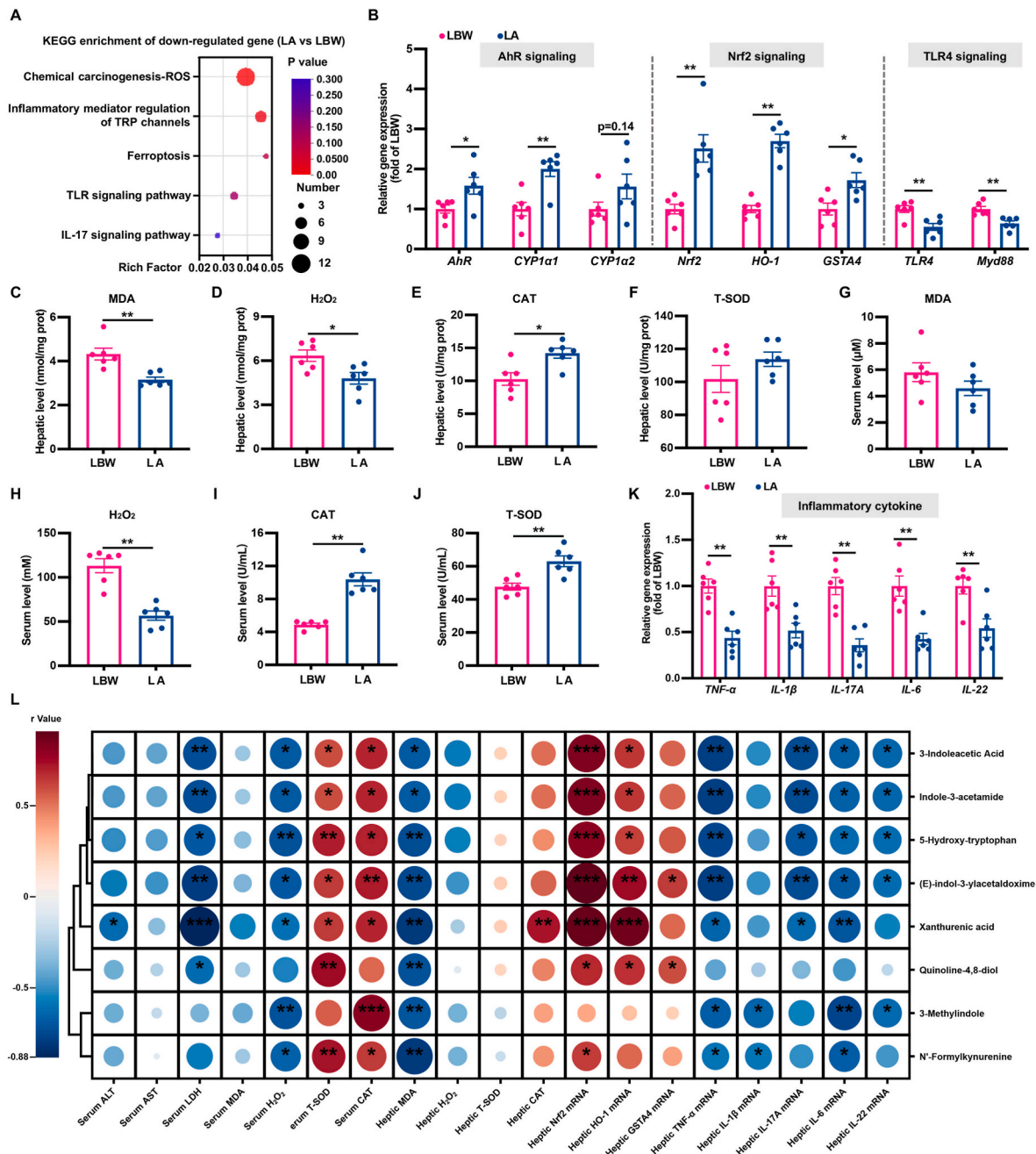
Fig. 8. AOS improved hepatic oxidative stress and inflammatory responses via activation of AhR signaling. (A) Hepatic KEGG enrichment of downregulated genes. (B) The relative levels of AhR, Nrf2, and TLR4 signaling. (C–F) Serum levels of MDA and H_2O_2 and activities of CAT and T-SOD. (G–J) Hepatic levels of MDA and H_2O_2 and activities of CAT and T-SOD. (K) The relative gene expression of $TNF-\alpha$, $IL-1\beta$, $IL-6$, $IL-22$, and $IL-17A$. GAPDH was used as a reference gene. (L) Spearman correlation between the relative abundance of tryptophan metabolites and indices for hepatic oxidative and inflammatory responses. Statistical significance was determined by Student's t-test, *P < 0.05, **P < 0.01.

Śliżewska, 2020; Mukherjee, Lordan, Ross, & Cotter, 2020), were significantly enriched and increased in AOS-treated LBW piglets. Other SCFA-producing bacteria were also induced by AOS. Correspondingly, AOS greatly increased the fecal levels of acetate, propionate, butyrate, valerate, isobutyrate, isovalerate, and total SCFAs. SCFAs are well known as energy sources for colonocytes and signal transduction molecules that maintain intestinal homeostasis by regulating redox status and inflammatory responses (Parada Venegas et al., 2019). Significant respective negative and positive correlations between SCFAs, pro-inflammatory cytokines and bacteria enriched in piglets in the LA group were also identified by Spearman correlation analysis. In particular, we found that Lactobacillus and L. amylovorus had significant linear

relationships with all the SCFAs. Thus, it is reasonable to speculate that AOS alleviated intestinal dysfunctions by promoting SCFAs and Lactobacillus.

The liver is responsible for energy homeostasis through the regulation of glucose and lipid metabolism (Jensen-Cody & Potthoff, 2021) and thus is the major organ affected by ROS generated during energy metabolism (S. Li, Tan, et al., 2015). We first investigated serum indices of hepatic damage and found that AOS decreased the elevated levels of AST, ALT, and LDH in LBW piglets, indicating the protective effects of AOS against hepatic damage. Mechanically, the protective effects of AOS were associated with attenuation of hepatic oxidative stress and inflammatory responses as revealed by KEGG enrichment analysis, serum

and hepatic oxidative indices, and mRNA levels of pro-inflammatory signaling. Several studies have reported hepatic lipid deposition, increased TG and TC levels, and insulin resistance which resulted in increased levels of glucose and insulin in LBW piglets (Niu, et al., 2019). Consistently, elevated TG and TC levels in the liver and serum and increased serum glucose, insulin, GLP-1, and HOMA-IR were observed in our study, which was in agreement with previous reports. Unsaturated AOS, sharing similar properties with the AOS used in our study, has been proven to decrease serum glucose, TG, TC, NEFA, AST, and ALT levels in high-fat-diet (HFD)-induced obesity of zebrafish and mice (S. Li et al., 2019; Tran, Cho, Kwon, & Kim, 2019). However, no previous study has reported the regulatory roles of AOS in IUGR-induced aberrant lipid and glucose metabolism in the postnatal period. Notably, AOS significantly abrogated the abovementioned increases in those indices, which suggested the potential of AOS in the regulation of hepatic lipid metabolism and insulin resistance.

In consideration that AOS showed hepatic protection and regulatory effects on glucose and lipid metabolism in LBW piglets but not in NBW piglets, we performed more in-depth analyses mainly between the LBW and LA groups. The hepatic transcriptome revealed that genes downregulated by AOS were mainly enriched in hepatic lipid metabolism. Uptake of circulatory lipids and *de novo* synthesis contribute to hepatic lipid accumulation (M. Li, Reynolds, et al., 2015). We found that AOS significantly reduced the mRNA levels of genes involved in FFA uptake. In particular, AOS decreased the mRNA levels of *chREBP*, *SREBP1c*, *LXRα*, *PPARα*, and *PPARγ*, all of which are crucial transcription factors involved in hepatic *de novo* lipogenesis (Hodson & Gunn, 2019; Lodhi, Wei, & Semenkovich, 2011). Similar reductions in the expressions of these genes were observed in positive outcomes of HFD- or IUGR-induced hepatic lipid accumulation after nutritional intervention (Fu, et al., 2022; He et al., 2015). However, genes involved in β-oxidation were not altered by AOS. These results indicated that AOS attenuated hepatic lipid accumulation by decreasing *de novo* lipogenesis rather than enhancing β-oxidation. Alleviation of insulin resistance improves insulin sensitivity, which activates insulin receptor and downstream signals to inhibit gluconeogenesis and facilitate glycogenesis, uptake, and consumption of circulatory glucose. LBW piglets treated with AOS exhibited attenuated uptake of circulatory glucose, glycogenesis, and glycolysis and enhanced gluconeogenesis in the liver in the current study. This was consistent with the decreased insulin level and inactivation of the hepatic insulin signaling pathway and might be the adaptive mechanism in the remission phase of IUGR-induced aberrant hepatic metabolism. Interestingly, decreased pyruvate metabolism and citrate cycle were also observed in the liver, which may result from reduced glycolysis. Furthermore, it has also been reported that LBW piglets with natural postnatal "catch-up" growth performance are primarily due to lipid accumulation in organs rather than muscle gain, which may lead to a greater risk of fatty liver and cardiovascular diseases (Kopec, Shekhawat, & Mhanna, 2017; Morrison, Duffield, Muhlhausler, Gentili, & McMillen, 2010). In the current study, we first verified the growth-promoting effects of AOS and subsequently identified that AOS inhibited hepatic lipid deposition and improved HDL-C and LDL-C, biomarkers of cardiovascular diseases, thus further supporting the beneficial roles of AOS in postnatal life. In addition, circulatory glucose and lipids can also be utilized by other organs or deposited in adipose tissue and skeletal muscle, which are directly relevant to growth performance along with protein deposition. MAOS with a DP of 2–4 and its chromium complex was reported to enhance glucose uptake by activating AMP-activated protein kinase (AMPK) signaling, thus effectively improving insulin sensitivity in C2C12 skeletal muscle cells (C. Hao et al., 2011). However, whether AOS shows regulatory roles in glucose, lipid, and amino acid metabolism in adipose tissue and skeletal muscle in LBW piglets still needs further investigation.

It has been reported that the protective effects of prebiotics on hepatic dysfunctions can be achieved through the regulation of the gut microbiota and microbial metabolites (H. Y. Li et al., 2021). In the current study, hepatic KEGG enrichment and topology analyses of the metabolome revealed that tryptophan metabolism was significantly enriched and affected by AOS. However, tryptophan metabolism was decreased, as revealed by the hepatic transcriptome, which indicated that the hepatic tryptophan metabolites were mainly derived from the gut microbiota. *Lactobacillus* is one of the main bacteria that catabolizes colonic tryptophan (Roager & Licht, 2018), whose relative abundance was upregulated by AOS in this study. We further identified 8 greatly upregulated tryptophan metabolites and markedly activated AhR signaling pathway in the liver of AOS-treated piglets. The literature has reported that activation of AhR by indole-3-acetic acid attenuated hepatic lipogenesis by downregulating the expression of *ACC*, *SREBP1*, and *PPARγ* (Ji, Gao, Chen, Yin, & Zhang, 2019), while hepatocyte-specific knockout of AhR accelerated HFD-induced hepatic steatosis (Wada, et al., 2016). In addition, tryptophan supplementation decreased serum glucose and TG levels in LBW piglets (Goodarzi, et al., 2021). The 8 upregulated tryptophan metabolites showed negative correlations with TG, TC, NEFA, glucose, insulin, and HOMA-IR in the liver or serum, showing the similar outcomes of AhR activation to the previous reports. Nevertheless, the regulatory roles of AhR in hepatic steatosis remain controversial, as activation of AhR exacerbated hepatic steatosis and AhR deficiency protected against HFD-induced steatosis (P. Lu et al., 2015; Xu et al., 2015). However, it is certain that activation of AhR alleviated hepatic oxidative stress and inflammatory responses (Carambia & Schuran, 2021; Dietrich, 2016), as shown by the significant positive or negative correlations of the 8 upregulated tryptophan metabolites with antioxidant or oxidative and pro-inflammatory indices presented in the current study.

5. Conclusion

Collectively, the current study demonstrated that AOS improved the growth performance of LBW piglets by alleviating aberrant activation of colonic mucosal immunity and hepatic lipid deposition and insulin resistance. Mechanically, as revealed by integrated multi-omics, AOS alleviated the disruption of colonic mucosal immunity by increasing the abundance of SCFAs and SCFA-producing bacteria while improved hepatic injury and lipid and glucose metabolism by increasing tryptophan metabolites and activation of AhR signaling. Our findings further verify AOS as a novel kind of prebiotic in the intestine, and show the promising potential of AOS for treating metabolic disorders in LBW mammals.

CRediT authorship contribution statement

Yunchang Zhang: Writing – original draft, Visualization, Project administration, Methodology, Investigation, Funding acquisition, Conceptualization. **Xiong Deng:** Resources, Investigation. **Tairan Liu:** Investigation, Formal analysis. **Baocheng Hu:** Validation, Investigation. **Baoyi Yu:** Investigation. **Linshu Jiang:** Writing – review & editing. **Zhenlong Wu:** Writing – review & editing. **Martine Schroyen:** Writing – review & editing. **Ming Liu:** Writing – review & editing, Supervision, Project administration, Funding acquisition.

Declaration of competing interest

The authors declare the following financial interests/personal relationships which may be considered as potential competing interests:

Ming Liu reports financial support was provided by The National Key Research and Development Program of China (2021YFD1301003).

Yunchang Zhang reports financial support was provided by Beijing Postdoctoral Research Foundation (2023-ZZ-119). If there are other authors, they declare that they have no known competing financial interests or personal relationships that could have appeared to influence the work reported in this paper.

Data availability

Data will be made available on request.

Appendix A. Supplementary data

Supplementary data to this article can be found online at https://doi.org/10.1016/j.foodhyd.2024.109980.

References

Ayuso, M., Irwin, R., Walsh, C., Van Cruchten, S., & Van Ginneken, C. (2021). Low birth weight female piglets show altered intestinal development, gene expression, and epigenetic changes at key developmental loci. *The FASEB Journal, 35*(4), Article e21522.

Bauer, R., Walter, B., Hoppe, A., Gaser, E., Lampe, V., Kauf, E., et al. (1998). Body weight distribution and organ size in newborn swine (sus scrofa domestica) – a study describing an animal model for asymmetrical intrauterine growth retardation. *Experimental & Toxicologic Pathology, 50*(1), 59–65.

Bechmann, L. P., Hannivoort, R. A., Gerken, G., Hotamisligil, G. S., Trauner, M., & Canbay, A. (2012). The interaction of hepatic lipid and glucose metabolism in liver diseases. *Journal of Hepatology, 56*(4), 952–964.

Bozzetti, V., Tagliabue, P. E., Visser, G. H., van Bel, F., & Gazzolo, D. (2013). Feeding issues in IUGR preterm infants. *Early Human Development, 89*(Suppl 2), S21–S23.

Brownlee, I. A., Allen, A., Pearson, J. P., Dettmar, P. W., Havler, M. E., Atherton, M. R., et al. (2005). Alginate as a source of dietary fiber. *Critical Reviews in Food Science and Nutrition, 45*(6), 497–510.

Carambia, A., & Schuran, F. A. (2021). The aryl hydrocarbon receptor in liver inflammation. *Seminars in Immunopathology, 43*(4), 563–575.

Chen, J., Song, Y., Chen, D., Yu, B., He, J., Mao, X., et al. (2021). Low birth weight disturbs the intestinal redox status and mitochondrial morphology and functions in newborn piglets. *Animals, 11*(9).

Chen, D., Wang, Y., Yu, L., Li, S. P., Zhao, H. M., Jiang, F. J., Wu, Y. X., et al. (2022). Maternal propionate supplementation ameliorates glucose and lipid metabolic disturbance in hypoxia-induced fetal growth restriction. *Food & Function, 13*(20), 10724–10736.

Cui, C., Wu, C., Wang, J., Ma, Z., Zheng, X., Zhu, P., et al. (2022). Restored intestinal integrity, nutrients transporters, energy metabolism, antioxidative capacity and decreased harmful microbiota were associated with IUGR piglet's catch-up growth before weaning. *Journal of Animal Science and Biotechnology, 13*(1), 129.

Dietrich, C. (2016). Antioxidant functions of the aryl hydrocarbon receptor. *Stem Cells International, 2016*, Article 7943495.

Falkeborg, M., Cheong, L. Z., Gianfico, C., Sztukiel, K. M., Kristensen, K., Glasius, M., et al. (2014). Alginate oligosaccharides: Enzymatic preparation and antioxidant property evaluation. *Food Chemistry, 164*, 185–194.

Fischer, A., & Wefers, D. (2019). Chromatographic analysis of alginate degradation by five recombinant alginate lyases from Cellulophaga algicola DSM 14237. *Food Chemistry, 299*, Article 125142.

Fu, X., Liu, Z., Li, R., Yin, J., Sun, H., Zhu, C., et al. (2022). Amelioration of hydrolyzed guar gum on high-fat diet-induced obesity: Integrated hepatic transcriptome and metabolome. *Carbohydrate Polymers, 297*, Article 100051.

Gheorghita Puscaselu, R., Lobiuc, A., Dimian, M., & Covasa, M. (2020). Alginate: From food industry to biomedical applications and management of metabolic disorders. *Polymers, 12*(10).

Goodarzi, P., Habibi, M., Roberts, K., Sutton, J., Shili, C. N., Lin, D., et al. (2021). Dietary tryptophan supplementation alters fat and glucose metabolism in a low-birthweight piglet model. *Nutrients, 13*(8).

Goodman, B. E. (2010). Insights into digestion and absorption of major nutrients in humans. *Advances in Physiology Education, 34*(2), 44–53.

Guilloteau, P., Zabielski, R., Hammon, H. M., & Metges, C. C. (2010). Nutritional programming of gastrointestinal tract development. Is the pig a good model for man? *Nutrition Research Reviews, 23*(1), 4–22.

Gustafsson, J. K., & Johansson, M. E. V. (2022). The role of goblet cells and mucus in intestinal homeostasis. *Nature Reviews Gastroenterology & Hepatology, 19*(12), 785–803.

Hao, Y., Fang, H., Yan, X., Shen, W., Liu, J., Han, P., et al. (2023). Alginate oligosaccharides repair liver injury by improving anti-inflammatory capacity in a busulfan-induced mouse model. *International Journal of Molecular Sciences, 24*(4).

Hao, C., Hao, J., Wang, W., Han, Z., Li, G., Zhang, L., et al. (2011). Insulin sensitizing effects of oligomannuronate-chromium (III) complexes in C2C12 skeletal muscle cells. *PLoS One, 6*(9), Article e24598.

He, J., Dong, L., Xu, W., Bai, K., Lu, C., Wu, Y., et al. (2015). Dietary tributyrin supplementation attenuates insulin resistance and abnormal lipid metabolism in suckling piglets with intrauterine growth retardation. *PLoS One, 10*(8), Article e0136848.

Hodson, L., & Gunn, P. J. (2019). The regulation of hepatic fatty acid synthesis and partitioning: The effect of nutritional state. *Nature Reviews Endocrinology, 15*(12), 689–700.

Houghton, D., Wilcox, M. D., Brownlee, I. A., Chater, P. I., Seal, C. J., & Pearson, J. P. (2019). Acceptability of alginate enriched bread and its effect on fat digestion in humans. *Food Hydrocolloids, 93*, 395–401.

Hsu, C. L., & Schnabl, B. (2023). The gut-liver axis and gut microbiota in health and liver disease. *Nature Reviews Microbiology, 21*(11), 719–733.

Huang, S. M., Wu, Z. H., Li, T. T., Liu, C., Han, D. D., Tao, S. Y., et al. (2020). Perturbation of the lipid metabolism and intestinal inflammation in growing pigs with low birth weight is associated with the alterations of gut microbiota. *Science of the Total Environment, 719*, Article 137382.

Jensen-Cody, S. O., & Potthoff, M. J. (2021). Hepatokines and metabolism: Deciphering communication from the liver. *Molecular Metabolism, 44*, Article 101138.

Ji, Y., Gao, Y., Chen, H., Yin, Y., & Zhang, W. (2019). Indole-3-Acetic acid alleviates nonalcoholic fatty liver disease in mice via attenuation of hepatic lipogenesis, and oxidative and inflammatory stress. *Nutrients, 11*(9).

Jiang, Z., Zhang, X., Wu, L., Li, H., Chen, Y., Li, L., et al. (2021). Exolytic products of alginate by the immobilized alginate lyase confer antioxidant and antiapoptotic bioactivities in human umbilical vein endothelial cells. *Carbohydrate Polymers, 251*, Article 116976.

Jones, J. G. (2016). Hepatic glucose and lipid metabolism. *Diabetologia, 59*(6), 1098–1103.

Kopec, G., Shekhawat, P. S., & Mhanna, M. J. (2017). Prevalence of diabetes and obesity in association with prematurity and growth restriction. *Diabetes, Metabolic Syndrome and Obesity, 10*, 285–295.

Li, S., He, N., & Wang, L. (2019). Efficiently anti-obesity effects of unsaturated alginate oligosaccharides (UAOS) in high-fat diet (HFD)-Fed mice. *Marine Drugs, 17*(9).

Li, N., Huang, S., Jiang, L., Wang, W., Li, T., Zuo, B., et al. (2018). Differences in the gut microbiota establishment and metabolome characteristics between low- and normal-birth-weight piglets during early-life. *Frontiers in Microbiology, 9*, 1798.

Li, M., Reynolds, C. M., Segovia, S. A., Gray, C., & Vickers, M. H. (2015). Developmental programming of nonalcoholic fatty liver disease: The effect of early life nutrition on susceptibility and disease severity in later life. *BioMed Research International, 2015*, Article 437107.

Li, S., Tan, H. Y., Wang, N., Zhang, Z. J., Lao, L., Wong, C. W., et al. (2015). The role of oxidative stress and antioxidants in liver diseases. *International Journal of Molecular Sciences, 16*(11), 26087–26124.

Li, Y., Zhang, H., Su, W., Ying, Z., Chen, Y., Zhang, L., et al. (2018). Effects of dietary Bacillus amyloliquefaciens supplementation on growth performance, intestinal morphology, inflammatory response, and microbiota of intra-uterine growth retarded weanling piglets. *Journal of Animal Science and Biotechnology, 9*, 22.

Li, H. Y., Zhou, D. D., Gan, R. Y., Huang, S. Y., Zhao, C. N., Shang, A., et al. (2021). Effects and mechanisms of probiotics, prebiotics, synbiotics, and postbiotics on metabolic diseases targeting gut microbiota: A narrative review. *Nutrients, 13*(9).

Liu, Y., Azad, M. A. K., Kong, X., Zhu, Q., & Yu, Z. (2022). Dietary bile acids supplementation modulates immune response, antioxidant capacity, glucose, and lipid metabolism in normal and intrauterine growth retardation piglets. *Frontiers in Nutrition, 9*, Article 991812.

Liu, J., Yang, S., Li, X., Yan, Q., Reaney, M. J. T., & Jiang, Z. (2019). Alginate oligosaccharides: Production, biological activities, and potential applications. *Comprehensive Reviews in Food Science and Food Safety, 18*(6), 1859–1881.

Lodhi, I. J., Wei, X., & Semenkovich, C. F. (2011). Lipoexpediency: De novo lipogenesis as a metabolic signal transmitter. *Trends in Endocrinology and Metabolism, 22*(1), 1–8.

Lu, S., Na, K., Wei, J., Tao, T., Zhang, L., Fang, Y., et al. (2023). Alginate oligosaccharide structures differentially affect DSS-induced colitis in mice by modulating gut microbiota. *Carbohydrate Polymers, 312*, Article 120806.

Lu, P., Yan, J., Liu, K., Garbacz, W. G., Wang, P., Xu, M., et al. (2015). Activation of aryl hydrocarbon receptor dissociates fatty liver from insulin resistance by inducing fibroblast growth factor 21. *Hepatology, 61*(6), 1908–1919.

Mackie, A. R., Macierzanka, A., Aarak, K., Rigby, N. M., Parker, R., Channell, G. A., et al. (2016). Sodium alginate decreases the permeability of intestinal mucus. *Food Hydrocolloids, 52*, 749–755.

Markowiak-Kopeć, P., & Śliżewska, K. (2020). The effect of probiotics on the production of short-chain fatty acids by human intestinal microbiome. *Nutrients, 12*(4).

Matthews, D. R., Hosker, J. P., Rudenski, A. S., Naylor, B. A., Treacher, D. F., & Turner, R. C. (1985). Homeostasis model assessment: Insulin resistance and beta-cell function from fasting plasma glucose and insulin concentrations in man. *Diabetologia, 28*(7), 412–419.

McMillen, I. C., & Robinson, J. S. (2005). Developmental origins of the metabolic syndrome: Prediction, plasticity, and programming. *Physiological Reviews, 85*(2), 571–633.

Morrison, J. L., Duffield, J. A., Muhlhausler, B. S., Gentili, S., & McMillen, I. C. (2010). Fetal growth restriction, catch-up growth and the early origins of insulin resistance and visceral obesity. *Pediatric Nephrology, 25*(4), 669–677.

Mukherjee, A., Lordan, C., Ross, R. P., & Cotter, P. D. (2020). Gut microbes from the phylogenetically diverse genus Eubacterium and their various contributions to gut health. *Gut Microbes, 12*(1), Article 1802866.

Mutamba, A. K., He, X., & Wang, T. (2022). Therapeutic advances in overcoming intrauterine growth restriction induced metabolic syndrome. *Frontiers in Pediatrics, 10*, Article 1040742.

Neu, J., & Zhang, L. (2005). Feeding intolerance in very-low-birthweight infants: What is it and what can we do about it? *Acta Paediatrica - Supplement, 94*(449), 93–99.

Niu, Y., He, J., Zhao, Y., Shen, M., Zhang, L., Zhong, X., et al. (2019). Effect of curcumin on growth performance, inflammation, insulin level, and lipid metabolism in weaned piglets with IUGR. *Animals, 9*(12).

Parada Venegas, D., De la Fuente, M. K., Landskron, G., González, M. J., Quera, R., Dijkstra, G., et al. (2019). Short chain fatty acids (SCFAs)-Mediated gut epithelial and immune regulation and its relevance for inflammatory bowel diseases. *Frontiers in Immunology, 10*.

Postic, C., Dentin, R., & Girard, J. (2004). Role of the liver in the control of carbohydrate and lipid homeostasis. *Diabetes & Metabolism, 30*(5), 398–408.

Rao, Y., Kuang, Z., Li, C., Guo, S., Xu, Y., Zhao, D., et al. (2021). Gut Akkermansia muciniphila ameliorates metabolic dysfunction-associated fatty liver disease by regulating the metabolism of L-aspartate via gut-liver axis. *Gut Microbes, 13*(1), 1–19.

Roager, H. M., & Licht, T. R. (2018). Microbial tryptophan catabolites in health and disease. *Nature Communications, 9*(1), 3294.

Romo, A., Carceller, R., & Tobajas, J. (2009). Intrauterine growth retardation (IUGR): Epidemiology and etiology. *Pediatric Endocrinology Reviews, 6*(Suppl 3), 332–336.

Roura, E., Koopmans, S. J., Lallès, J. P., Le Huerou-Luron, I., de Jager, N., Schuurman, T., et al. (2016). Critical review evaluating the pig as a model for human nutritional physiology. *Nutrition Research Reviews, 29*(1), 60–90.

Roy, S., & Dhaneshwar, S. (2023). Role of prebiotics, probiotics, and synbiotics in management of inflammatory bowel disease: Current perspectives. *World Journal of Gastroenterology, 29*(14), 2078–2100.

Stojanov, S., Berlec, A., & Štrukelj, B. (2020). The influence of probiotics on the firmicutes/bacteroidetes ratio in the treatment of obesity and inflammatory bowel disease. *Microorganisms, 8*(11).

Sundaram, S., & Borthakur, A. (2021). Altered intestinal epithelial nutrient transport: An underappreciated factor in obesity modulated by diet and microbiota. *Biochemical Journal, 478*(5), 975–995.

Tran, V. C., Cho, S. Y., Kwon, J., & Kim, D. (2019). Alginate oligosaccharide (AOS) improves immuno-metabolic systems by inhibiting STOML2 overexpression in high-fat-diet-induced obese zebrafish. *Food & Function, 10*(8), 4636–4648.

Wada, T., Sunaga, H., Miyata, K., Shirasaki, H., Uchiyama, Y., & Shimba, S. (2016). Aryl hydrocarbon receptor plays protective roles against high fat diet (HFD)-induced hepatic steatosis and the subsequent lipotoxicity via direct transcriptional regulation of Socs3 gene expression. *Journal of Biological Chemistry, 291*(13), 7004–7016.

Wan, J., Zhang, J., Chen, D., Yu, B., Mao, X., Zheng, P., et al. (2018). Alginate oligosaccharide-induced intestinal morphology, barrier function and epithelium apoptosis modifications have beneficial effects on the growth performance of weaned pigs. *Journal of Animal Science and Biotechnology, 9*, 58.

Wan, J., Zhang, J., Xu, Q., Yin, H., Chen, D., Yu, B., et al. (2021). Alginate oligosaccharide protects against enterotoxigenic Escherichia coli-induced porcine intestinal barrier injury. *Carbohydrate Polymers, 270*, Article 118316.

Wang, X., Lin, G., Liu, C., Feng, C., Zhou, H., Wang, T., et al. (2014). Temporal proteomic analysis reveals defects in small-intestinal development of porcine fetuses with intrauterine growth restriction. *The Journal of Nutritional Biochemistry, 25*(7), 785–795.

Wellington, M. O., Rodrigues, L. A., Li, Q., Dong, B., Panisson, J. C., Yang, C., et al. (2021). Birth weight and nutrient restriction affect jejunal enzyme activity and gene markers for nutrient transport and intestinal function in piglets. *Animals, 11*(9).

Wu, G., Bazer, F. W., Wallace, J. M., & Spencer, T. E. (2006). Board-invited review: Intrauterine growth retardation: Implications for the animal sciences. *Journal of Animal Science, 84*(9), 2316–2337.

Xu, C. X., Wang, C., Zhang, Z. M., Jaeger, C. D., Krager, S. L., Bottum, K. M., et al. (2015). Aryl hydrocarbon receptor deficiency protects mice from diet-induced adiposity and metabolic disorders through increased energy expenditure. *International Journal of Obesity, 39*(8), 1300–1309.

Yao, W., Kong, Q., You, L., Zhong, S., & Hileuskaya, K. (2023). Polysaccharides from brown seaweed: Physicochemical properties, absorption in the intestine, and beneficial effects on intestinal barrier. *Food Frontiers, 4*(4), 1547–1560.

Zhang, W., Ma, C., Xie, P., Zhu, Q., Wang, X., Yin, Y., et al. (2019). Gut microbiota of newborn piglets with intrauterine growth restriction have lower diversity and different taxonomic abundances. *Journal of Applied Microbiology, 127*(2), 354–369.

Zhao, Y., Yu, S., Zhao, H., Li, L., Li, Y., Tu, Y., et al. (2022). Lipidomic profiling using GC and LC-MS/MS revealed the improved milk quality and lipid composition in dairy cows supplemented with citrus peel extract. *Food Research International, 161*, Article 111767.